Magnetic properties and magnetocaloric effects of $RNiSi_2$ (R= Gd, Dy, Ho, Er, Tm) compounds

B. Zhang, X. Q. Zheng, Y. Zhang, X. Zhao, J. F. Xiong, S. L. Zuo, D. Liu, T. Y. Zhao, F. X. Hu, and B. G. Shen

Citation: AIP Advances **8**, 056423 (2018); doi: 10.1063/1.5007018
View online: https://doi.org/10.1063/1.5007018
View Table of Contents: http://aip.scitation.org/toc/adv/8/5
Published by the American Institute of Physics

AIP ADVANCES **8**, 056423 (2018)

Magnetic properties and magnetocaloric effects of $RNiSi_2$ (R= Gd, Dy, Ho, Er, Tm) compounds

B. Zhang,[1,2] X. Q. Zheng,[3] Y. Zhang,[1,2] X. Zhao,[1,2] J. F. Xiong,[1,2] S. L. Zuo,[1,2] D. Liu,[1,2] T. Y. Zhao,[1,2] F. X. Hu,[1,2] and B. G. Shen[1,2,a]

[1]*State Key Laboratory of Magnetism, Institute of Physics, Chinese Academy of Sciences, Beijing, China*

[2]*University of Chinese Academy of Sciences, Beijing, China*

[3]*School of Materials Science and Engineering, University of Science and Technology Beijing, Beijing, China*

(Presented 8 November 2017; received 29 September 2017; accepted 17 November 2017; published online 4 January 2018)

Orthorhombic $CeNiSi_2$-type polycrystalline $RNiSi_2$ (R=Gd, Dy, Ho, Er, Tm) compounds were synthesized and the magnetic and magnetocaloric properties were investigated in detail. The transition temperatures of $RNiSi_2$ compounds are all in a very low temperature range (<30 K). As temperature increases, all of the compounds undergo an AFM to PM transition ($GdNiSi_2$ at 18 K, $DyNiSi_2$ at 25 K, $HoNiSi_2$ at 10.5 K, $ErNiSi_2$ at 3 K and $TmNiSi_2$ at 3.5 K, respectively). $ErNiSi_2$ compound shows the largest $(\Delta S_M)_{max}$ (maximal magnetic entropy change) among these compounds. The value of $(\Delta S_M)_{max}$ is 27.9 J/kgK under a field change of 0-5 T, which indicates that $ErNiSi_2$ compound is very competitive for practical applications in low-temperature magnetic refrigeration in the future. $DyNiSi_2$ compound shows large inverse MCE (almost equals to the normal MCE) below the T_N which results from metamagenitic transition under magnetic field. Considering of the normal and inverse MCE, $DyNiSi_2$ compound also has potential applications in low-temperature multistage refrigeration. https://doi.org/10.1063/1.5007018

I. INTRODUCTION

The magnetocaloric effect (MCE), a kind of physical phenomenon found more than 130 years ago, is one of the intrinsic properties of magnetic materials. Commercial and residential refrigeration, based on conventional gas compression/expansion technology, is a mature industry. However, the magnetic refrigeration (MR) based on MCE is becoming competitive with conventional gas compression/expansion technology because its environmental friendliness and high efficiency.[1–5] In the last twenty years great progress has been made on exploring large MCE materials for applications at room temperature such as refrigerators and air conditioners.[6,7] The typical room temperature MCE materials mainly include $Gd_5Si_2Ge_2$,[8,9] $La(Fe, Si)_{13}$,[10–14] $MnAs_{1-x}Sb_x$,[15] $MnFeP_{1-x}As_x$,[16] Heusler alloys,[17,18] etc. MCE materials are generally evaluated by the following parameters: the maximum value of magnetic entropy change ($(\Delta S_M)_{max}$), the full width at half maximum of $\Delta S_M - T$ curve (δT_{FWHM}), refrigerant capacity (RC) and adiabatic temperature change (ΔT_{ad}). For most MCE materials, the value of the ΔS_M is negative (normal MCE). But the positive ΔS_M which called inverse MCE also can be found in some materials such as $TbNiGe_2$,[19] $TbMn_{0.33}Ge_2$,[20] etc. Recently, much attention has also been paid on the MCE materials with low transition temperature because these materials are promising to be used for gas liquefaction in magnetic cooling cycle or combined magnetic-gas cooling cycle.[6,21] These low temperature MCE materials mainly include the rare earth based intermetallic compounds such as RCo_2,[22,23] RNi,[24] etc.

[a]Corresponding author: shenbaogen@yeah.net

Rare earth based intermetallic compounds have shown interesting magnetic properties and excellent performance on MCE. The ternary $RTSi_2$ series (R is rare earth, T is transition metal) is one category of rare earth based intermetallic compounds which has been intensively studied during the last decades.[25–27] The results show that the compounds with R= Pr and Nd are ferromagnets and those with R= Gd, Tb, Dy, Ho, Er are antiferromagnets. Experimental results of electrical resistivity, Hall coefficient, magnetic susceptibility and specific heat for $CeNiSi_2$ support a theory of the Anderson lattice.[28] Neutron diffraction and magnetic measurements on $RNiSi_2$ compounds where R= Pr and Nd give refined atomic position parameters and it is found that the preferred moment direction is along the c axis.[29] The same measurements on $RNiSi_2$ compounds where R= Tb, Dy, Ho, Er show that the compounds all have uniaxial moment arrangements and have almost the same easy axis, the shortest axis c, except for $ErNiSi_2$ with an easy axis of a axis.[30–33]

Considering the lack of research work on MCE of $RNiSi_2$ compounds, further study on magnetic properties and MCE will be performed. In this paper, the polycrystalline $RNiSi_2$ (R=Gd, Dy, Ho, Er, Tm) compounds were synthesized. The magnetic properties and MCE which both contains normal and inverse effects were investigated in detail.

II. EXPERIMENTAL PROCEDURE

The polycrystalline $RNiSi_2$ (R=Gd, Dy, Ho, Er, Tm) compounds were prepared by arc-melting appropriate proportion of constituent components with the purity better than 99.9% in a water-cooled copper hearth in a high-purity argon atmosphere. The ingots were turned over after each melting and re-melted several times to ensure the compositional homogeneity. After arc-melting, the ingots were wrapped by molybdenum foil respectively and sealed in a high-vacuum quartz tube, annealed at 1273K for 25 days, finally quenched into liquid nitrogen. The crystal structure was characterized by powder X-ray diffraction (XRD) method with Cu Kα radiation. Magnetic measurements including the temperature dependence of magnetization (M-T) and the field dependence of magnetization (M-H) curves were performed by employing Vibrating Sample Magnetometer with Quantum Design (SQUID-VSM). Heat capacity measurements were carried out by employing Physical Properties Measurement System (PPMS).

III. RESULTS AND DISCUSSION

The XRD pattern of $RNiSi_2$ (R=Gd, Dy, Ho, Er, Tm) compounds at room temperature and its crystal structure are shown in Fig. 1. Almost all of the diffraction peaks can be indexed to an

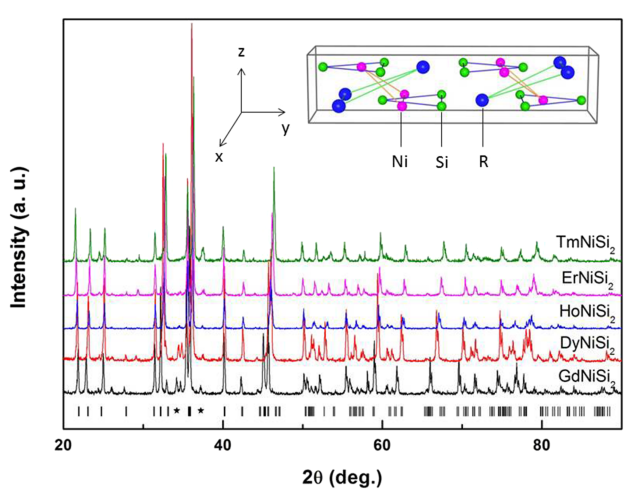

FIG. 1. The XRD patterns of $RNiSi_2$ (R= Gd, Dy, Ho, Er, Tm) compounds measured at room temperature. The inset is the crystal structure of $RNiSi_2$.

orthorhombic $CeNiSi_2$-type structure (space group Cmcm #63). The result is in accord with previous work.[26] The Bragg positions are marked at the bottom of the picture. It can also be seen that there is a small peak around 37.5° for all compounds and a peak around 34.5° for $GdNiSi_2$ and $DyNiSi_2$ compound, which indicates that small amount of impurity may exist. The impurity is indexed as $RNiSi_3$. However, it does not affect our discussions and conclusions because the amount of impurity is not large. As the atom number of R increases, the position of diffraction peaks moves towards higher angle range, which indicates that the lattice constant becomes smaller from $GdNiSi_2$ to $TmNiSi_2$ compound.

The Zero-Field-Cooled (ZFC) and Field-Cooled (FC) magnetization curves for $RNiSi_2$ compounds were measured under a field of 0.01 T. They are shown in Fig. 2(a)–(d). The MH curves for $RNiSi_2$ compounds are also shown in Fig. 2(e)–(h). The MT for $DyNiSi_2$ shows a rapid increase and then a decrease with the increasing temperature, which indicates that this compound undergoes a simple transition from antiferromagnetic (AFM) to paramagnetic (PM) phase. The same conclusion can also be found in MH curves. The transition temperature is determined to be T_N=25 K. The overlap of ZFC and FC curves around T_N shows a good thermal reversibility in this compound. From MH curve we can see the compound occurs metamagenetic transition with the field increasing. All of the features mentioned above can also be found in other compounds. The transition temperatures along with the effective magnetic moments, which have been calculated according to the Curie-Weiss Law, are shown in Table I. The effective moment and ion moment is almost the same for each compound, indicating only rare earth atoms contribute to the magnetic moments in this series of compounds. It reveals from Fig. 2 that the value of the transition temperature (T_N) shows a decreasing trend when the atomic number of rare earth atom increases. However, there is an exception for $TmNiSi_2$, which may result from the complex magnetic coupling in $TmNiSi_2$ compound.

The MCE materials are generally evaluated by isothermal magnetic entropy change (ΔS_M), which is calculated from isothermal magnetization data (M-H curves) by using Maxwell relation: $\Delta S_M = \int_0^H (\partial M/\partial T)_H dH$. The temperature dependences of ΔS_M under a field change of 0-2 T and 0-5 T for $RNiSi_2$ compounds are shown in Fig. 3(a)–(d), respectively. The results shows that all compounds show normal MCE because the value of ΔS_M is negative around transition temperatures

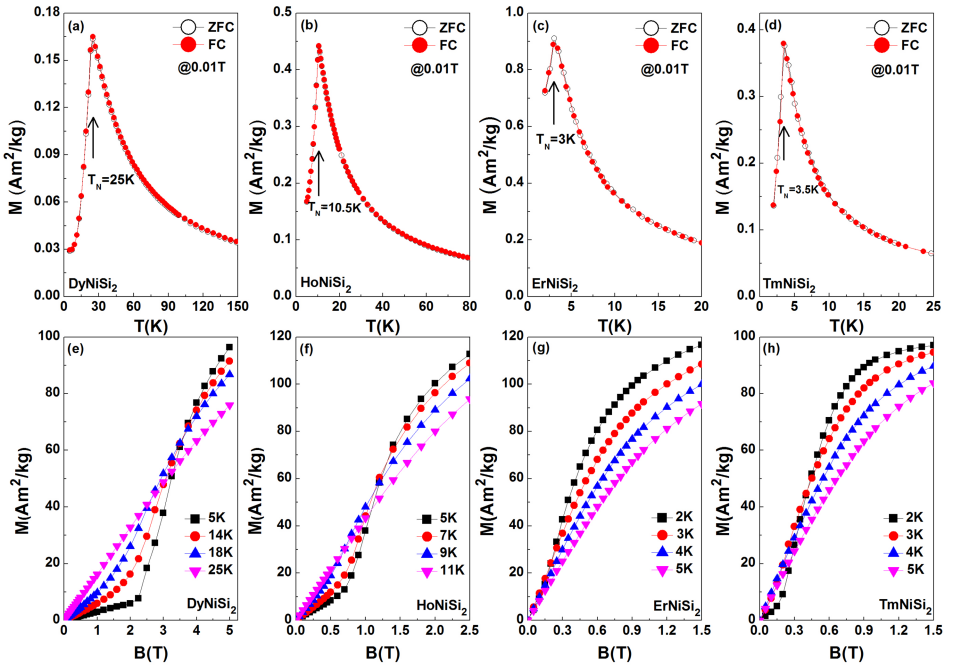

FIG. 2. The MT and MH curves of $RNiSi_2$ (R= Dy, Ho, Er, Tm) compounds, respectively. (a) MT for $DyNiSi_2$. (b) MT for $HoNiSi_2$. (c) MT for $ErNiSi_2$. (d) MT for $TmNiSi_2$. (e) MH for $DyNiSi_2$. (f) MH for $HoNiSi_2$. (g) MH for $ErNiSi_2$. (h) MH for $TmNiSi_2$.

TABLE I. The transition temperatures, effective magnetic moments, ion magnetic moments and magnetocaloric parameters of $RNiSi_2$ (R= Gd, Dy, Ho, Er, Tm) compounds and other compounds.

				0-2T			0-5T		
Materials	$T_N(K)$	$M_{eff}(\mu_B)$	$M_{ion}(\mu_B)$	$-(\Delta S_M)_{max}$ $(J/kg\ K)$	$\delta T_{FWHM}(K)$	$RC(J/kg)$	$-(\Delta S_M)_{max}$ $(J/kg\ K)$	$\delta T_{FWHM}(K)$	$RC(J/kg)$
$GdNiSi_2$	18.0	8.2	7.8	0.7	20.2	9.9	3.5	21.2	58.0
$DyNiSi_2$	25.0	10.7	10.5	0.7	15.3	8.6	4.4	15.8	59.0
$DyNiSi_2$	-	-	-	(-2.5)	-	31.6	(-3.6)	-	90.5
$HoNiSi_2$	10.5	11	10.6	5.3	8.9	35.4	16.8	15.6	198.8
$ErNiSi_2$	3.0	9.1	9.6	17.0	-	75.8	27.9	-	225.3
$TmNiSi_2$	3.5	7.0	7.1	12.3	7.5	71.2	16.4	17.2	222.6
$ErMn_2Si_2$[34]	4.5	-	-	20.0	-	130	25.2	-	365
TmCuAl[35]	2.8	-	-	17.2	-	129	24.3	-	372
$ErNi_2Si_2$[36]	3.5	-	-	15.1	-	-	22.9	-	-
ErNiSi[37]	3.2			8.8			19.1		309

for each of them. However, $HoNiSi_2$ shows small inverse MCE below the transition temperature and $DyNiSi_2$ shows large inverse MCE (almost equals to the normal MCE) below the transition temperature which will be discussed in detail in the following section. It can be observed from Fig. 3 that all of the curves have a large peak and the maximal magnetic entropy change ($(\Delta S_M)_{max}$) occurs around T_N. The refrigerant capacity (RC) is another important parameter to evaluate MCE materials. The value of RC can be calculated by using the approach $RC = \int_{T_1}^{T_2} |\Delta S_M| dT$, where T_1 and T_2 are the temperatures corresponding to the full width at the half value of $(\Delta S_M)_{max}$, respectively. And we call $\delta T_{FWHM} = T_2 - T_1$ the refrigerant temperature width. The $(\Delta S_M)_{max}$, RC and δT_{FWHM} of $RNiSi_2$ compounds under a field change of 0-2 T and 0-5 T are calculated and shown in Table I. The MCE parameters of some low temperature MCE materials are also shown in Table I for comparison.[34–37] For $ErNiSi_2$ compound, the value of $(\Delta S_M)_{max}$ is 17.0 J/kgK for 0-2 T and 27.9 J/kgK for 0-5 T

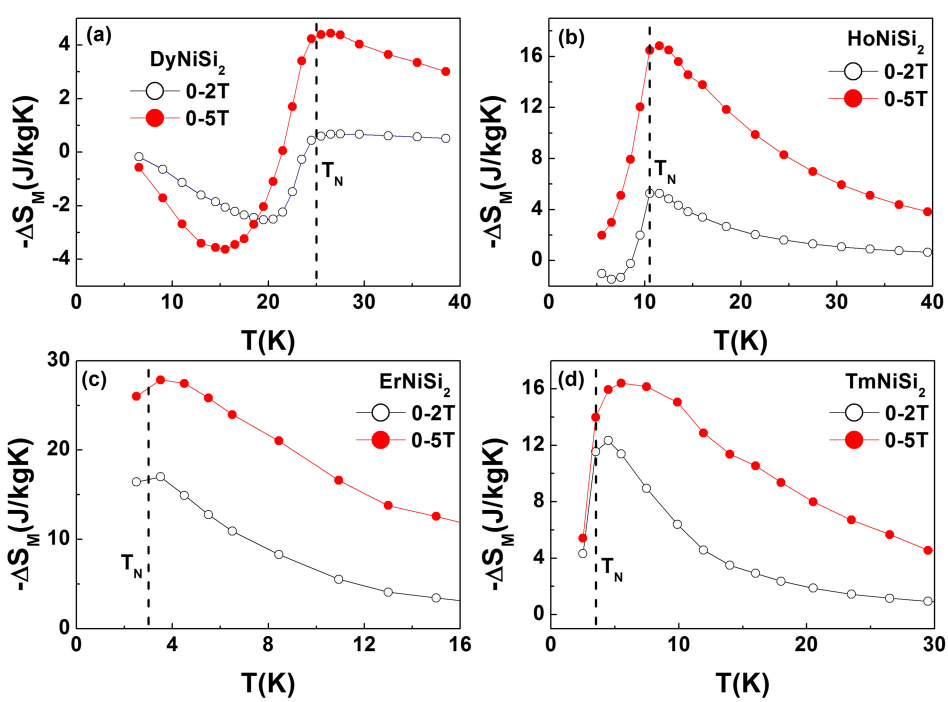

FIG. 3. The temperature dependences of ΔS_M at a field change of 0-2 T and 0-5 T for $RNiSi_2$ (R= Dy, Ho, Er, Tm) compounds, respectively. (a) $DyNiSi_2$. (b) $HoNiSi_2$. (c) $ErNiSi_2$. (d) $TmNiSi_2$.

respectively, which are comparable or even larger than those of other listed materials. The RC of $ErNiSi_2$ compound is approximately calculated to be 75.8 J/kg for 0-2 T and 225.3 J/kg for 0-5 T, respectively, where the integration starts with the temperature of 2 K. These values are not accurate because the actual low temperature boundary of δT_{FWHM} is far lower than 2 K for ErNiSi2 compound. According to the model proposed by Oesterrreicher et al.[38] The $(\Delta S_M)_{max}$ is positively correlated with the total angular momentum quantum number (J) and negatively correlated with magnetic ordering temperature. In this series, $HoNiSi_2$ compound shows the largest J, but its Neel temperature is much larger than that of $ErNiSi_2$ compound. Considering that $HoNiSi_2$ and $ErNiSi_2$ have a similar J, the value of Neel temperature exerts a main effect on the value of $(\Delta S_M)_{max}$. As a result, $ErNiSi_2$ compound shows the largest $(\Delta S_M)_{max}$ among $RNiSi_2$ compounds. The excellent MCE performance of $ErNiSi_2$ compound indicates its potential applications in low temperature refrigeration.

The Fig. 3 also shows that $DyNiSi_2$ and $HoNiSi_2$ compounds both have positive ΔS_M below T_N, which called inverse MCE. This phenomenon results from the mixed exchange interaction and the applied magnetic field leads to a further spin-disordered state,[39] which occurs metamagenitic transition. This makes $\partial M/\partial T$ positive under T_N. For $HoNiSi_2$ compound, the positive ΔS_M can only be found under a low field change and the value of positive ΔS_M is far smaller than the absolute value of negative ΔS_M around T_N. When the field change is 5T, the positive ΔS_M has been disappeared, which indicates that the AFM ground state of $HoNiSi_2$ compound below T_N is relatively weak. The same phenomenon can also be found in many Heusler alloys and AFM magnetocaloric effect materials.[39] However, for $DyNiSi_2$ compound, the inverse MCE can even be found in a high field change such as 5T and the maximal positive ΔS_M is almost equals to the maximal negative ΔS_M. For further study, heat capacity was measured and ΔS_M also calculated using heat capacity data through the expression $\Delta S_M = \int_0^H \{[C(T,H) - C(T,0)]/T\}dT$. The results all shown in Fig. 4. The Fig. 4 shows that the curves obtained using magnetization data are in good agreement with the corresponding curves obtained using heat capacity. And the field change of the maximal positive ΔS_M occurs is about 3.6T. The large inverse MCE results from the strong AFM coupling in $DyNiSi_2$ compounds which may be related to the large magnetocrystalline anisotropy of Dy atoms. The inverse MCE can also be used for magnetic refrigeration if only the refrigerator works in a reverse process. For example, for $DyNiSi_2$ compound, magnetic refrigeration can be realized in a usual working recycle around 25K and it can be used in a reverse working recycle around 15K, which seems useful in multistage refrigeration. And the RC of $DyNiSi_2$ compound is re-calculated by considering of the contribution of inverse MCE at lower temperatures which also shown in Table I. The value of RC for a field change of 0–5 T is modified from 59 J/kg and 90.5 J/kg.

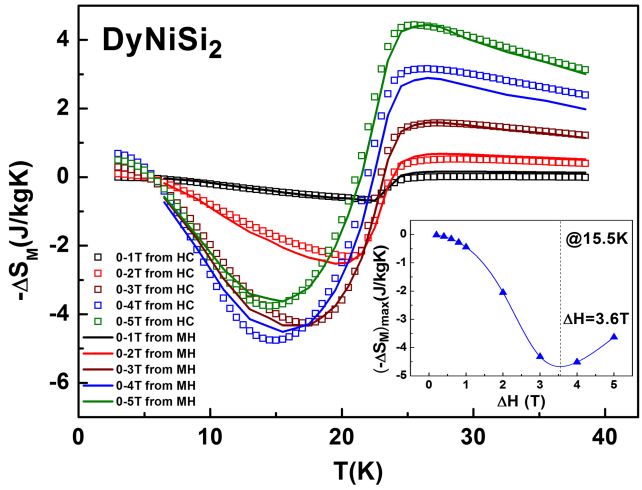

FIG. 4. The temperature dependences of ΔS_M for $DyNiSi_2$ compound calculated from magnetization and heat capacity data for field changes of 0-1T, 0-2T, 0-3T, 0-4T, and 0-5T, respectively. The inset shows the field change dependences of $(\Delta S_M)_{max}$ for inverse MCE at 15.5K.

The excellent performance of $DyNiSi_2$ compound indicates its potential applications in low temperature refrigeration.

IV. CONCLUSION

In summary, all orthorhombic $CeNiSi_2$-type polycrystalline $RNiSi_2$ (R=Gd, Dy, Ho, Er, Tm) compounds are AFM ordered and T_N in a very low temperature. Among these compounds, $ErNiSi_2$ compound shows the largest $(\Delta S_M)_{max}$ and RC, which is larger than almost all of the materials in this low temperature range, indicating its potential practical applications in low-temperature magnetic refrigeration in the future. $DyNiSi_2$ compound shows large inverse MCE (almost equals to the normal MCE) below the T_N which results from metamagenitic transition under magnetic field. Considering of the normal and inverse MCE, $DyNiSi_2$ compound also has potential applications in low-temperature multistage refrigeration.

ACKNOWLEDGMENTS

This work was supported by the National Key Research Program of China (Grant No. 2014CB643702, 2016YFB0700903), the National Natural Science Foundation of China (Grant No. 51590880) and the Knowledge Innovation Project of the Chinese Academy of Sciences (Grant No. KJZD-EW-M05).

[1] E. Brück, J. Phys. D. Appl. Phys. **38**, R381 (2005).
[2] K. A. Gschneidner and V. K. Pecharsky, Annu. Rev. Mater. Sci. **30**, 387 (2000).
[3] X. Moya, S. Kar-Narayan, and N. D. Mathur, Nat. Mater. **13**, 439 (2014).
[4] V. K. Pecharsky and K. A. Gschneidner, Jr., J. Magn. Magn. Mater. **200**, 44 (1999).
[5] A. M. Tishin and Y. I. Spichkin, The Magnetocaloric Effect and Its Applications (2003).
[6] K. A. Gschneider, Jr., V. K. Pecharsky, and A. O. Tsokol, Reports Prog. Phys. **68**, 1479 (2005).
[7] B. G. Shen, J. R. Sun, F. X. Hu, H. W. Zhang, and Z. H. Cheng, Adv. Mater. **21**, 4545 (2009).
[8] V. K. Pecharsky and K. A. Gschneidner, Jr., Phys. Rev. Lett. **78**, 4494 (1997).
[9] A. Giguère, M. Foldeaki, B. Ravi Gopal, R. Chahine, T. K. Bose, A. Frydman, and J. A. Barclay, Phys. Rev. Lett. **83**, 2262 (1999).
[10] A. Fujita, S. Fujieda, Y. Hasegawa, and K. Fukamichi, Phys. Rev. B **67**, 104416 (2003).
[11] A. Fujita, Y. Akamatsu, and K. Fukamichi, J. Appl. Phys. **85**, 4756 (1999).
[12] F. X. Hu, B. G. Shen, and J. R. Sun, Appl. Phys. Lett. **80**, 826 (2002).
[13] F. X. Hu, B. G. Shen, J. R. Sun, Z. H. Cheng, G. H. Rao, and X. X. Zhang, Appl. Phys. Lett. **78**, 3675 (2001).
[14] B.-G. Shen, F.-X. Hu, Q.-Y. Dong, and J.-R. Sun, Chinese Phys. B **22**, 17502 (2013).
[15] H. Wada and Y. Tanabe, Appl. Phys. Lett. **79**, 3302 (2001).
[16] O. Tegus, E. Brück, K. H. J. Buschow, and F. R. de Boer, Nature **415**, 150 (2002).
[17] F. Hu, B. Shen, J. Sun, and G. Wu, Phys. Rev. B **64**, 132412 (2001).
[18] J. Liu, T. Gottschall, K. P. Skokov, J. D. Moore, and O. Gutfleisch, Nat. Mater. **11**, 620 (2012).
[19] S. Gupta, K. G. Suresh, A. V. Lukoyanov, Yu. V. Knyazev, and Yu. I. Kuz'min, J. Alloys Compd. **664**, 120 (2016).
[20] S. Gupta and K. G. Suresh, Physica B **448**, 260 (2014).
[21] H. Yayama, Y. Hatta, Y. Makimoto, and A. Tomokiyo, Jpn. J. Appl. Phys. **39**, 4220 (2000).
[22] N. H. Duc and D. T. K. Anh, J. Magn. Magn. Mater. **242**, 873 (2002).
[23] A. Giguere, M. Foldeaki, W. Schnelle, and E. Gmelin, J. Phys. Condens. Matter **11**, 6969 (1999).
[24] X. Q. Zheng, B. Zhang, H. Wu, F. X. Hu, Q. Z. Huang, and B. G. Shen, J. Appl. Phys. **120**, 163907 (2016).
[25] A. Gil, A. Szytula, Z. Tomkowicz, K. Wojciechowski, and A. Zygmunt, Acta Phys. Pol. A **85**, 271 (1994).
[26] A. Gil, A. Szytuła, Z. Tomkowicz, K. Wojciechowski, and A. Zygmunt, J. Magn. Magn. Mater. **129**, 271 (1994).
[27] V. Ivanov, L. Vinokurova, and A. Szytula, J. Alloys Compd. **218**, L24 (1995).
[28] E. D. Mun, Y. S. Kwon, and M. H. Jung, Phys. Rev. B **67**, 33103 (2003).
[29] P. Schobinger-Papamantellos and K. H. J. Buschow, J. Alloys Compd. **185**, 51 (1992).
[30] P. Schobinger-Papamantellos and K. H. J. Buschow, J. Less Common Met. **171**, 321 (1991).
[31] P. Schobinger-Papamantellos, C. Ritter, and K. H. Buschow, J. Alloys Compd. **264**, 89 (1998).
[32] P. Schobinger-Papamantellos, F. Fauth, and K. H. J. Buschow, J. Alloys Compd. **252**, 50 (1997).
[33] P. Schobinger-Papamantellos, K. H. J. Buschow, C. Wilkinson, F. Fauth, and C. Ritter, J. Magn. Magn. Mater. **189**, 214 (1998).
[34] L. Li, K. Nishimura, W. D. Hutchison, Z. Qian, D. Huo, and T. Namiki, Appl. Phys. Lett. **100**, 152403 (2012).
[35] Z. J. Mo, J. Shen, L. Q. Yan, J. F. Wu, L. C. Wang, J. Lin, C. C. Tang, and B. G. Shen, Appl. Phys. Lett. **102**, 192407 (2013).
[36] W. Zuo, F. Hu, S. Jirong, and B. Shen, J. Magn. Magn. Mater. **344**, 96 (2013).
[37] S. Gupta, R. Rawat, and K. G. Suresh, Appl. Phys. Lett. **105**, 012403 (2014).
[38] H. Oesterreicher and F. T. Parker, J. Appl. Phys. **55**, 4334 (1984).
[39] T. Krenke, E. Duman, M. Acet, E. F. Wassermann, X. Moya, L. Mañosa, and A. Planes, Nat. Mater. **4**, 450 (2005).